LASERS AND AMPLIFIRES

PACS numbers: 42.55.Rz; 42.60.Lh; 42.65.Re
DOI: 10.1070/QE2001v031n08ABEH002028

Prospects for the development of femtosecond laser systems based on beryllium aluminate crystals doped with chromium and titanium ions*

E V Pestryakov, A I Alimpiev, V N Matrosov

***Abstract*. The physical and laser properties of beryllium-containing $BeAl_2O_4$, $BeAl_6O_{10}$, $Be_3Al_2Si_6O_{18}$, and $BeLaAl_{11}O_{19}$ oxide crystals doped with chromium and titanium ions are studied. The $Cr^{3+}:BeAl_2O_4$, $Cr^{3+}:BeAl_6O_{10}$, and $Ti^{3+}:BeAl_2O_4$ crystals were shown to compare favourably in physical and laser properties with the well-known laser media and to be candidates for femtosecond laser systems.**

Keywords: *femtosecond lasers, solid-state active media, impurity ions.*

1. Introduction

Considerable recent progress has been achieved in the field of generation of ultrashort laser pulses. Optical pulses of duration 4.5 fs were obtained, which corresponds approximately to two oscillation cycles of the optical field [1]. Compact high-power femtosecond laser systems based on chirped-pulse amplification (CPA) were built [2, 3], which produce light fluxes with an intensity up to 10^{20} W cm^{-2} [4 – 6]. All these achievements are related to a great extent to the use of solid-state active media doped with impurity ions with vibronic amplification bands [7].

In the majority of contemporary femtosecond laser systems, Ti^{3+}-doped sapphire crystals ($Ti:Al_2O_3$) are employed. This active medium possesses a relatively large stimulated-emission cross section along with an extremely broad vibronic amplification band in the 650 – 1050 nm region and a very high thermal conductivity, which is comparable with that of copper at low temperatures [7]. All this makes a $Ti:Al_2O_3$ crystal a highly efficient medium for the generation and amplification of ultrashort laser pulses and for the development of terawatt femtosecond laser systems, including those operating with a kilohertz pulse repetition rate [8, 9].

In addition, femtosecond laser systems based on other active media are also actively developed. These media include $Cr^{4+}:Mg_2SiO_4$ forsterite crystals [10, 11], the $Cr^{3+}:LiCaAlF_6$, $Cr^{3+}:LiSrAlF_6$, and $Cr^{3+}:LiSrGaAlF_6$ crystals [12, 13], and glasses and crystals doped with Yb^{3+} ions [14]. Compared to $Ti:Al_2O_3$, these media exhibit higher quantum efficiencies. In addition, they can be pumped by semiconductor laser diodes, which significantly improves the efficiency of a laser system as a whole. However, all of them have narrower amplification bands and lower thermal conductivities than the $Ti:Al_2O_3$ crystal.

Schemes combining different laser media in master femtosecond lasers and amplifying stages permit the efficient use of the advantages of different doped crystals [4]. An analysis of the potentialities of the active media for the production of terawatt femtosecond laser systems and lasers emitting extremely short pulses calls for a comprehensive investigation of the basic parameters, which determine the capacity of the crystal matrices and the active ions to generate and amplify femto- and subfemtosecond laser pulses.

In this paper, we considered the possibility of using beryllium-containing oxide crystals of the $pBeO - mAl_2O_3 - nSiO_2$ series – $BeAl_2O_4$ chrysoberyl, $BeAl_6O_{10}$ beryllium hexaaluminate, $Be_3Al_2Si_6O_{18}$ beryl, and $BeLaAl_{11}O_{19}$ beryllium–lanthanum hexaaluminate crystals – as Cr^{3+} and Ti^{3+}-doped laser media. The Cr^{3+}-doped beryl and beryllium hexaaluminate crystals were shown to be candidates for the amplifying stages of femtosecond laser systems and the Ti^{3+}-doped chrysoberyl crystal for the generation of ultrashort pulses.

2. Specific features of spectral properties of active media for femtosecond lasers

To efficiently produce and amplify ultrashort pulses, the active media of femtosecond laser systems should possess specific properties. The parameters of the media, which determine these properties, can be divided into two groups: the spectral-lasing and thermal physical parameters. The spectral and lasing properties play the most important role, because they determine the specific features of femtosecond pulse generation and amplification. Note that the requirements on these properties are determined both by the ultrashort-pulse parameters and physical processes employed in the production and amplification of these pulses.

*Based on the report presented at the Seminar on Ultrafast Processes in Substances and Laser Femtotechnologies (Nizhnii Novgorod, Institute of Applied Physics, Russian Academy of Sciences, 7 – 8 December, 2000)

E V Pestryakov Institute of Laser Physics, Siberian Division, Russian Academy of Sciences, prosp. Lavrent'eva 13/3, 630090 Novosibirsk, Russia; e-mail: pefvic@laser.nsc.ru
A I Alimpiev Design and Technology Institute of Monocrystals, Siberian Division, Russian Academy of Sciences, ul. Russkaya 43, 630058 Novosibirsk, Russia;
V N Matrosov Belorussian State Polytechnical Academy, Partizanskii prosp. 74, 220600 Minsk-107, Belarus; e-mail: solix@belsonet.net

Received 24 April 2001
Kvantovaya Elektronika **31** (8) 689 – 696 (2001)
Translated by E N Ragozin

At present, ultrashort pulses are generated in cw solid-state lasers primarily by producing the soliton regime upon a combined action of self-amplitude and self-phase modulation due to the intracavity Kerr lens and the compensation for the group velocity dispersion produced by dispersive elements [15, 16].

Amplification bands of the active media in lasers operating by the mechanism of Kerr-lens mode-locking (KML lasers) should be first of all broad enough to generate femtosecond pulses. Moreover, the active medium of a KML laser should provide the gain required for the realisation of the Kerr mode-locking mechanism.

Analysis of the optimal conditions for Kerr-lens mode-locking performed in Refs [17–19] showed that the efficiency of mode-locking depends on many parameters and to determine it, the data are required on the active medium, and also the parameters of the laser cavity, as well as on its nonlinear and dispersive elements. For a conventional Z-shaped cavity geometry of a KML Ti : Al_2O_3 crystal laser, calculations yield the required intracavity power of the order of $10^5 - 10^6$ W [16].

The ratio between the bandwidth $\Delta\nu$ and the gain $g(\nu)$ of a laser required for producing such powers can be obtained in the maximum-inversion approximation. In this case, $g(\nu) \approx \sigma(\nu)N$ for the vibronic transition, where $\sigma(\nu)$ is the emission cross section and N is the concentration of active centres. Let us analyse the relation between $g(\nu)$ and $\Delta\nu$ using the relation between $g(\nu)$ and $\Delta\nu$. For a Gaussian profile of the vibronic luminescence band, the emission cross section at the maximum of the amplification band is [20]

$$\sigma(\nu_{\max}) = \frac{2}{8\pi}\left(\frac{\ln 2}{\pi}\right)^{1/2}\frac{\lambda^2}{n^2}\frac{g_1}{g_2}\frac{1}{\Delta\nu_{\text{eff}}\tau}, \quad (1)$$

where $\Delta\nu_{\text{eff}}$ is the effective width of the emission band related to the luminescence intensity I_{em} by the expression

$$\Delta\nu_{\text{eff}} = 2\left(\frac{\ln 2}{\pi}\right)^{1/2}\frac{\int I_{\text{em}}(\nu)\mathrm{d}\nu}{I_{\text{em}}(\nu_{\max})}; \quad (2)$$

g_i are the statistical weights of the upper ($i = 2$) and lower ($i = 1$) levels; n is the index of refraction; τ is radiative lifetime; and $I_{\text{em}}(\nu_{\max})$ is the luminescence intensity at the maximum.

This basic relation between the main spectral parameters of the active medium can be represented as $\sigma(\nu_{\max}) = M_{\text{am}}\lambda^2/(\tau\Delta\nu_{\text{eff}}n^2)$, where

$$M_{\text{am}} = \sigma(\nu_{\max})\tau\Delta\nu_{\text{eff}}(n/\lambda)^2 = (2/8\pi)(\ln 2/\pi)^{1/2} = 0.0374 \quad (3)$$

is a constant common to all solid-state laser media with Gaussian luminescence bands and $g_1 = g_2$.

Expression (3) permits one to determine from a given pulse duration τ_{p} the relation between the lifetime and the emission cross section of the active medium required for the generation of a pulse of a given duration. To produce a transform-limited pulse of the soliton type of duration $\tau_{\text{p}} = 10$ fs, the amplification bandwidth should be no less than $\Delta\nu_{\text{eff}} = 1000$ cm^{-1}. From expression (3) it follows that for the active medium with $n = 1.76$ and $\lambda = 800$ nm, we have $\sigma(\nu_{\max})\tau = 7.7 \times 10^{-25}$ cm^2 s, i.e., for the excited-state lifetime $\tau = 3$ μs, the emission cross section should be $\sigma(\nu_{\max}) = 2.57 \times 10^{-19}$ cm^2. This value agrees well with the cross section $\sigma(\nu_{\max})$ for the $^2E - {}^2T_2$ vibronic transition of the Ti^{3+} ion in a sapphire crystal [7]. Note that the cross section $\sigma_{\text{esa}}(\nu)$ for absorption from the excited state in the spectral amplification region was not included in the analysis. In some cases, this absorption can narrow down the amplification region, and the effective emission cross section $\sigma_{\text{eff}}(\nu) = \sigma(\nu) - \sigma_{\text{esa}}(\nu)$ should then be considered [21].

Upon amplification of ultrashort pulses by the chirped-pulse method, the main parameter that characterises the efficiency of the active medium in CPA laser systems is the limiting amplified radiation intensity I_{m} (theoretical peak power per square centimeter) [22]. Taking into account expression (3), this parameter has the form

$$I_{\text{m}} = \Delta\nu_{\text{eff}}h\nu/\sigma(\nu) = 4\pi(\pi/\ln 2)^{1/2}(n/hc)^2(h\nu)^3\tau\Delta\nu_{\text{eff}}^2. \quad (4)$$

Based on relationships (3) and (4), we can state that the requirement common to the active media upon CPA and KML generation of femtosecond pulses is that the width of the amplification band $\Delta\nu_{\text{eff}}$ should be large. To generate femtosecond pulses in KML lasers, it is important to have the emission cross section large enough to obtain a high intensity and realise the Kerr-lens mode-locking with the formation of a soliton regime. At the same time, obtaining the limiting peak intensities in CPA lasers requires, conversely, moderate values of the emission cross section to exclude any limitations on the saturation energy upon CPA.

In accordance with expression (3), active media with long excited-level lifetimes satisfy to a greater extent the latter condition. For this reason, crystals and glasses doped not only with ions of the iron group (Ti, Cr, etc., or 3*d* ions, i.e., ions with the unfilled *d* electron shell), but also with ions of the lanthanide group (Nd, Yb, etc., or 4*f* ions) are promising for the development of terawatt CPA laser systems. Because of the specific features of the electron shell filling, the amplification bands of ions of the lanthanide group are narrower and, as a rule, excited-state lifetimes for these ions are long. For instance, for the Yb^{3+} ion in crystals and glasses, $\tau \approx 1$ ms. This ion also has a very high quantum efficiency $\eta = \lambda_{\text{ab}}/\lambda_{\text{em}}$, which can be as high as 0.98 in some media. However, the width of the emission band does not exceed 100 cm^{-1} even in disordered crystal matrices and glasses, and therefore the minimum duration of ultrashort pulses for Yb^{3+}-doped media is about of 100 fs [14].

The methods for generation of pulses shorter than 10 fs hold the greatest interest today [4–6]. To generate 10-fs and shorter pulses, the width of the amplification band should exceed 1000 cm^{-1}. This condition can be fulfilled by using solid-state matrices doped with *d* ions. Note that it is difficult to obtain stimulated emission in ions of this type because their upper unfilled shell is not virtually covered by other electron shells, as for *f* ions, resulting in a strong dependence of its properties on the environment of an impurity ion in the matrix. In the case of a strong electron–phonon interaction, spectral transitions are strongly broadened, leading to the formation of broad vibronic emission bands that are appropriate for ultrashort pulse amplification [7, 20, 23–25].

In the single configurational coordinate model (Fig. 1) [24], the dependence of the width $\Delta\nu$ of the amplification band on the crystal field parameters of the active medium determined by the electron–phonon interaction is described by the expression

$$\Delta\nu = 2\left(\frac{2\hbar}{m_{\text{e}}\omega_{\text{ph}}}\right)^{1/2} m\omega_{\text{ph}}^2 Q_0$$

$$= \frac{70}{16}(21\pi)^{-1/2}\left(\frac{2\hbar\omega_e}{m_e\omega_e^2}\right)^{1/2}(Ze)^{2/5}\langle r^4\rangle^{1/5}\mathrm{Dq}^{-1/5}. \quad (5)$$

Expression (5) was derived in a single-mode approximation for the phonon spectrum assuming that $S_g\hbar\omega_g = S_e\hbar\omega_e = S\hbar\omega_{ph}$ and taking into account that for an octahedrally coordinated ion in the active medium, the displacement Q_0, the crystal field parameter Dq and the Huang – Rhys factor S [20, 24] are related as

$$10\mathrm{Dq} = E_{ab} = \frac{350}{16}(21\pi)^{-1/2}(Ze)\langle r^4\rangle/Q_0^5, \quad (6)$$

$$S\hbar\omega_{ph} = \frac{1}{2}(E_{ab} - E_{em}) = \frac{1}{2}m_e\omega_{ph}^2Q_0^2, \quad (7)$$

where Ze is the effective ion charge; r is the effective ion radius; ω_{ph} is the effective phonon frequency; $\omega_{g,e}^2 = k_{g,e}/m_{g,e}$; $k_{g,e} = \mathrm{d}^2U_{g,e}/\mathrm{d}Q^2$; $m_{g,e}$ is the effective oscillator mass in the ground (g) and excited (e) states; $U_g(Q)$ and $U_e(Q)$ are the potential curves of the ground and excited states; and Q is the configurational coordinate (Fig. 1). The parameter S gives the number of lattice photons $\hbar\omega_{ph}$ involved in the electron – phonon interaction and is a quantitative measure of the electron – phonon interaction [20, 24].

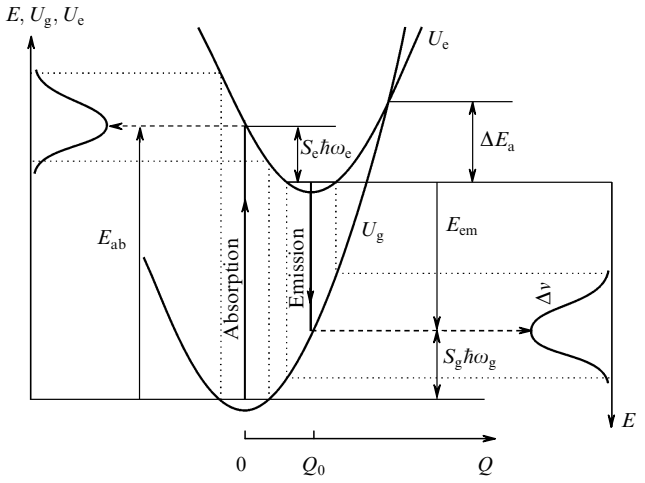

Figure 1. Optical transitions between two nondegenerate states in the configuration-coordinate diagram of an impurity ion.

In this model, the limiting displacement Q_0 at which the emission on the transition is still observed, is determined by the relation

$$10\mathrm{Dq} > 4S\hbar\omega_{ph} = 2m\omega_{ph}^2Q_0^2, \quad (8)$$

and the nonradiative losses are determined by the activation energy (Fig. 1)

$$\Delta E_a = \frac{(10\mathrm{Dq} - 2S\hbar\omega_{ph})^2}{4S\hbar\omega_{ph}} = \frac{10\mathrm{Dq} - 2m\omega_{ph}^2Q_0^2}{4m\omega_{ph}^2Q_0^2}. \quad (9)$$

Expressions (3) – (8) show that to obtain broad emission bands, crystals with a weak crystal field should be used. In this case, the maximum of the ion emission spectrum will shift to the red and the luminescence band will broaden proportionally to $\mathrm{Dq}^{-1/5}$.

As for the thermal physical properties of the active media of KML and CPA lasers, laser media with high thermal physical parameters are required for the efficient removal of heat released in the active element due to Stokes and other linear and nonlinear losses. This is particularly important for high-power lasers and systems operating at a kilohertz pulse repetition rate [8, 9].

To quantitatively determine whether the thermal physical properties of an active medium allow its use in KML and CPA laser systems, the thermal strength parameter [26]

$$R_t = \chi S_t(1 - \nu_P)(E\alpha)^{-1}, \quad (10)$$

can be employed. Here, χ, S_t, E, ν_P, and α are the thermal conductivity coefficient, the tensile strength, the Young modulus, the Poisson coefficient, and the coefficient of linear thermal expansion, respectively. As noted above, the sapphire crystal ranks highest in this parameter R_t. The high value of R_t for sapphire (Table 1) is one of the advantages of this medium, which led to its wide use in chirped-pulse amplifiers operating at kilohertz pulse repetition rates.

Along with sapphire, a high thermal strength is inherent in many beryllium-containing oxide crystals. Note that virtually all beryllium aluminate crystals, whose family also includes alexandrite, exhibit good thermal physical characteristics [27 – 30], because their basis is formed by two $p\mathrm{BeO} - m\mathrm{Al_2O_3}$ oxides, whose excellent thermal physical properties are well known [26].

Based on the above relations for the spectral and thermal physical parameters of the active media of femtosecond lasers, we analysed the efficiency of laser media which gained the widest acceptance in the production of KML and CPA laser systems. These parameters are presented in Table 1 for the three best known laser media. Considering the entire set of parameters of significance for CPA laser systems, one can see that alexandrite crystals surpass even $\mathrm{Ti:Al_2O_3}$ crystals, all the more Cr : forsterite crystals.

Taking into account the relation between the spectral characteristics of impurity ions and the crystal field parameters of solid-state matrices and considering the excellent thermal physical properties of oxide beryllium-containing compounds, we suppose that crystals of the $p\mathrm{BeO} - m\mathrm{Al_2O_3} - n\mathrm{SiO_2}$ family are promising for fabricating new laser media with broad emission bands for the amplification and generation of femtosecond pulses in KML and CPA lasers.

3. Active media for femtosecond lasers based on Cr- and Ti-doped beryllium aluminate crystals

3.1 Spectral properties of Cr and Ti ions

Among compounds of the $p\mathrm{BeO} - m\mathrm{Al_2O_3} - n\mathrm{SiO_2}$ series, $\mathrm{BeAl_2O_4}$ chrysoberyl, $\mathrm{BeAl_6O_{10}}$ beryllium hexaaluminate, $\mathrm{Be_3Al_2Si_6O_{18}}$ beryl, and $\mathrm{BeLaAl_{11}O_{19}}$ beryllium – lanthanum hexaaluminate crystals were grown. The beryl crystals were grown by the hydrothermal and gas-transport techniques. The remaining crystals were grown by the Czochralski technique on facilities with induction heating.

Table 1. Physical and spectral characteristics of several known oxide laser crystals.

Characteristic	Cr^{4+}:Mg_2SiO_4 [10, 11, 32–34]	Ti^{3+}:Al_2O_3 [7, 26, 35]	Cr^{3+}:$BeAl_2O_4$ [26, 27, 35]
Density ρ/g cm^{-3}	3.22	3.99	3.69
Mohs hardness	7	9	8.5
Heat capacity c_p/J g^{-1} K^{-1}	0.74	0.75	0.83
Thermal conductivity coefficient χ/W m^{-1} K^{-1}	5	42	23
Young modulus $E/10^9$ N m^{-2}	210*	405*	446*
Poisson coefficient ν_P	0.24*	0.25*	0.3*
Linear expansion coefficient $\alpha/10^{-6}$ K^{-1}	9.5	5.0–6.0	6.0–7.0
Tensile strength $S_t/10^6$ N m^{-2}	220	440	520
Thermal strength parameter R_t/W m^{-1}	420	5700	3100
Lasing bandwidth $\Delta\lambda$/nm	1130–1400	700–1050	700–790
Amplification bandwidth $\Delta\nu$/cm^{-1}	1700	3800	1650
Wavelength at the maximum of the amplification band λ/nm	1240	785	750
Emission cross section σ_{eff} (10^{-19} cm^2)	1.15	2.77	0.07
Metastable-level lifetime τ/μs			
$T = 77$ K	25	3.85	–
$T = 300$ K	2.7	3.0	260
Index of refraction n	1.63	1.76	1.74
Nonlinear index $n_2/10^{-16}$ cm^2 W^{-1}	2.0	3.2	2.9
Loss coefficient in the lasing region/cm^{-1}	0.01*	0.001*	0.005*
Limiting radiation intensity I_m/T W cm^{-2}	71	104	1876

*Note: Data obtained with crystals grown by V N Matrosov.

The results of investigation of the physical properties of beryllium aluminate crystals are presented in Table 2. They show that all crystals under investigation possess, as expected, excellent thermal physical parameters, the $BeAl_2O_4$ and $BeAl_6O_{10}$ ranking highest. Because the physical and structural properties of the beryllium hexaaluminate crystal are close to those of chrysoberyl, it may be referred to as 'pseudochrysoberyl'.

The spectral characteristics of Cr and Ti ion-doped crystals are shown in Figs 2–5. The absorption, luminescence excitation, and luminescence spectra are typical of octahedral-coordinated trivalent Cr and Ti ions.

A characteristic feature of the excitation spectra of Ti-doped crystals (Fig. 4) is the splitting of the upper excited ^2E state due to the Jahn–Teller effect [31], which is strongest for Ti ions in the $BeAl_6O_{10}$ crystal. The strong Jahn–Teller interaction is responsible for the splitting and the shift of the split components of the upper potential curve of the ion relative to the lower one, resulting in an additional broadening of the emission band. The maximum width of the amplification band for Ti ions is observed in the $BeAl_6O_{10}$

Table 2. Physical characteristics of beryllium-containing oxides.

Characteristic	$BeLaAl_{11}O_{19}$	$Be_3Al_2Si_6O_{18}$	$BeAl_6O_{10}$
Density ρ/g cm^{-3}	4.17	2.68	3.74
Mohs hardness	7	7.5	8.5
Heat capacity c_p/J g^{-1} K^{-1}	0.7	0.84	0.8
Thermal conductivity coefficient χ/W m^{-1} K^{-1}	10	5.6	12.5
Young modulus $E/10^9$ N m^{-2}	379	200	381
Poisson coefficient ν_P	0.24	0.24	0.24
Linear expansion coefficient $\alpha/10^{-6}$ K^{-1}	6.0 $\|\|a$	2.6 $\|\|c$	6.8 $\|\|a$
Melting temperature T/°C	1850	1470	1830

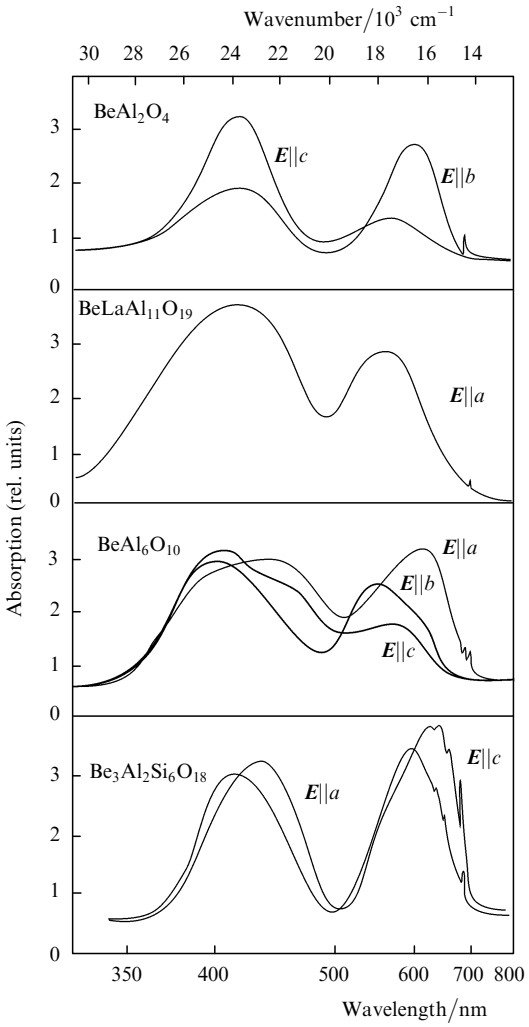

Figure 2. Absorption spectra of Cr^{3+} ions.

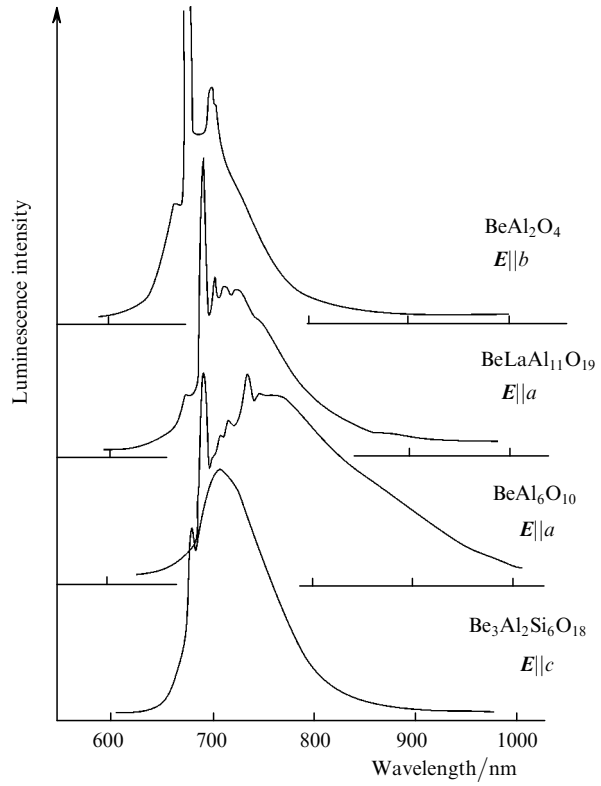

Figure 3. Luminescence spectra of Cr^{3+} ions.

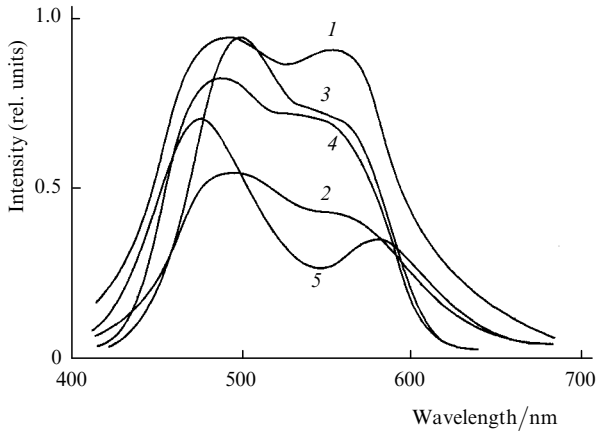

Figure 4. Excitation spectra of Ti^{3+} ions in $Be_3Al_2Si_6O_{18}$ (*1*), $BeLaAl_{11}O_{19}$ (*2*), $BeAl_2O_4$ (*3*), Al_2O_3 (*4*), and $BeAl_6O_{10}$ (*5*) crystals.

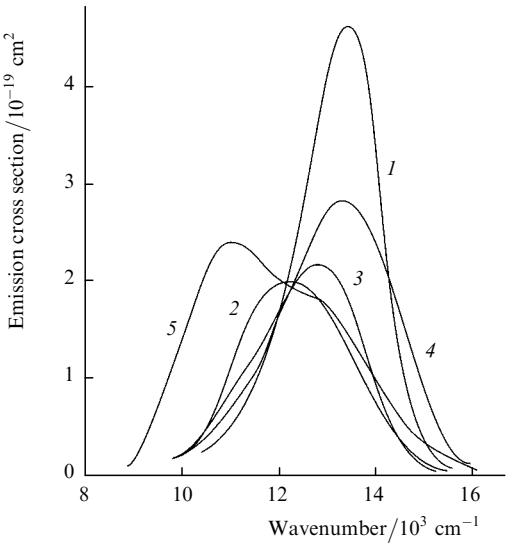

Figure 5. Effective emission cross section of Ti^{3+} ions in $Be_3Al_2Si_6O_{18}$ (*1*), $BeLaAl_{11}O_{19}$ (*2*), $BeAl_2O_4$ (*3*), Al_2O_3 (*4*), and $BeAl_6O_{10}$ (*5*) crystals.

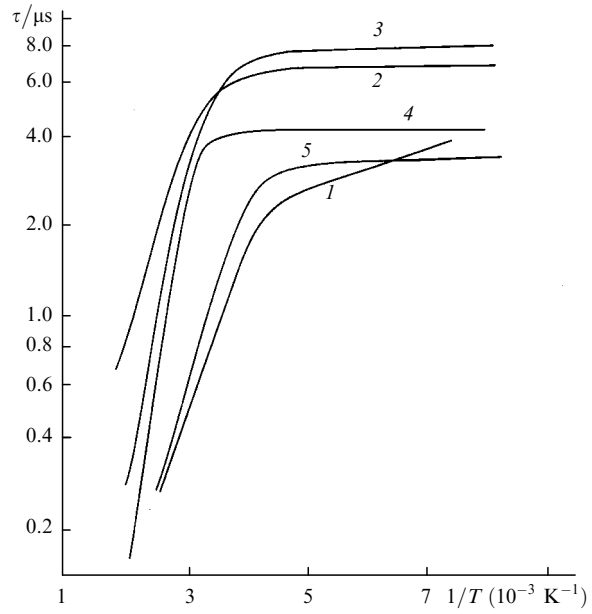

Figure 6. Temperature dependence of the lifetime of the excited state of Ti^{3+} ions in $Be_3Al_2Si_6O_{18}$ (*1*), $BeLaAl_{11}O_{19}$ (*2*), $BeAl_2O_4$ (*3*), Al_2O_3 (*4*), and $BeAl_6O_{10}$ (*5*) crystals.

crystal, it exceeds the width of a similar band in the Ti:sapphire crystal by nearly a factor of 1.5. The spectral dependence of the emission cross section for the $^2E - ^2T_2$ vibronic transition of Ti^{3+} ions in the $BeAl_6O_{10}$ crystal (Fig. 5) shows that titanium ions in this crystal experience a strong Jahn–Teller interaction both in the excited and ground states. This manifests itself in the characteristic double-humped shape of the spectral curve arising from the Jahn–Teller splitting of the ground state.

The temperature dependences of the excited-state lifetimes of titanium ions, given in Fig. 6, show that the activation energy ΔE_a is maximum for Ti in the chrysoberyl crystal and is close to ΔE_a in sapphire. In the remaining crystals, the activation energy is lower, indicating an increase in nonradiative losses with decreasing the crystal field parameter Dq. For the same reason it is possible to trace a trend towards broadening of the emission band in going over from the $BeAl_2O_4$ crystal to $BeAl_6O_{10}$, which is related to the increase in the electron–phonon interaction.

The spectral and lasing characteristics of the Cr^{3+} and Ti^{3+} ions in beryllium aluminate crystals are presented in Tables 3 and 4, respectively.

3.2 Lasing properties of the Cr^{3+} ion

The lasing properties of Cr^{3+}-doped crystals were investigated upon pulsed flashlamp excitation into the $^4A_2 - ^4T_2$ (510–690 nm) and $A_2 - ^4T_1$ (380–480 nm) absorption bands. The pumping was performed with xenon flashlamps made of fused quartz doped with cerium ions. Cerium ions improve the pumping efficiency of Cr^{3+} ions by converting

Table 3. Spectral and lasing characteristics of Cr^{3+} ions.

Characteristic	$BeLaAl_{11}O_{19}$	$Be_3Al_2Si_6O_{18}$	$BeAl_6O_{10}$
Luminescence range/nm	690 – 890	690 – 900	690 – 1000
Wavelength of the luminescence maximum/nm	730	720	770
Index of refraction n	1.79	1.56	1.735
Metastable-level lifetime (for $T = 300$ K) τ/μs	10	60	13.5
Transition cross section $\sigma/10^{-20}$ cm^2	1.0	3.4	6.0
Lasing range $\Delta\lambda$/nm	–	720 – 850	780 – 950
Limiting radiation intensity I_m/TW cm^{-2}	–	400	551

the UV radiation of flashlamps to the radiation in the absorption region of the $^4A_2 - {}^4T_1$ absorption band. This allowed us to obtain a differential efficiency of about 1 % at the centre of amplification bands of the $Cr:BeAl_2O_4$ (750 nm) and $Cr:BeAl_6O_{10}$ (830 nm) crystal lasers with a cavity containing a TF-8 glass dispersion prism. The dependences of the output energy for each of these lasers on the pump energy are plotted in Fig. 7, and the spectral dependences of the gain are given in Fig. 8. Note that even when the flashlamp pump pulse duration was not optimal (100 μs) with respect to the excited-state lifetime (13.5 μs), a rather high efficiency of lasing and a very broad amplification band, located in the region from 780 to 920 nm, were obtained in a $Cr:BeAl_6O_{10}$ laser.

The experimental data observed upon flashlamp excitation suggest that by optimising the pump duration and employing laser diode pumping at 650 nm, we can achieve a quantum efficiency η determined only by the Stokes losses: $\eta = 650$ nm/830 nm = 78 % for $Cr:BeAl_6O_{10}$ and $\eta = 650$ nm/750 nm = 87 % for $Cr:BeAl_2O_4$. We emphasise that for diode pumping, the most promising is a $Cr:BeAl_6O_{10}$ crystal which can be easily doped with Cr^{3+} ions at high concentrations without a significant sacrifice in the optical quality. Also among the advantages of this crystal is the fact that its $^4A_2 - {}^4T_2$ absorption band is shifted to the red relative to the absorption band of the $Cr:BeAl_2O_4$ crystal, allowing the use of diodes emitting at 670 nm for pumping.

A cw lasing upon pumping an argon laser (at 488 and 514.5 nm) was obtained in $Cr:Be_3Al_2Si_6O_{18}$ and $Cr:BeAl_6O_{10}$ crystals in a nonselective spherical cavity. Chromium ions were excited into the short-wavelength wing of the $^4A_2 - {}^4T_2$ absorption band, which is not very efficient for

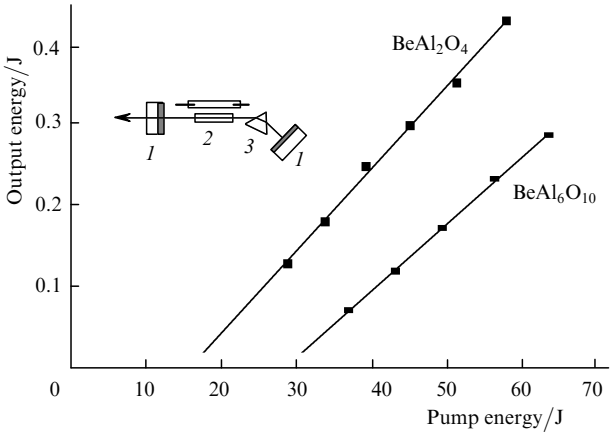

Figure 7. Dependences of the output energy on the pump energy for $Cr^{3+}:BeAl_2O_4$ (750 nm) and $Cr^{3+}:BeAl_6O_{10}$ (830 nm) lasers and the experimental setup: (*1*) mirrors; (*2*) doped crystal; (*3*) dispersion prism.

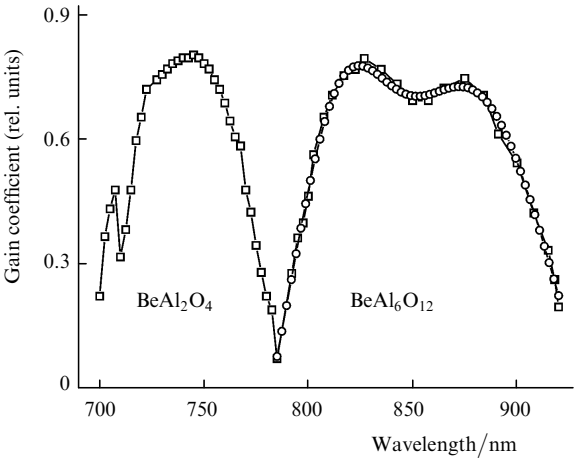

Figure 8. Amplification profiles for flashlamp-pumped $Cr^{3+}:BeAl_2O_4$ and $Cr^{3+}:BeAl_6O_{10}$ lasers.

Cr^{3+} ions. We also obtained lasing in $Cr:Be_3Al_2Si_6O_{18}$ ($\lambda = 765$ nm) and $Cr:BeAl_6O_{10}$ ($\lambda = 810$ nm) crystal lasers at a threshold pump intensity of 0.5 W. The high quality of $Cr:Be_3Al_2Si_6O_{18}$ crystals grown by the hydrothermal technique makes them promising for laser systems pumped by laser diodes emitting at 650 or 670 nm.

3.3 Lasing properties of the Ti^{3+} ion

Stimulated emission of Ti^{3+} ions was obtained only in $BeAl_2O_4$ crystals, whose optical quality ensured relatively low losses in the 700 – 1000 nm range. The crystals of other

Table 4. Spectral and lasing characteristics of Ti^{3+} ions.

Characteristic	$BeLaAl_{11}O_{19}$	$Be_3Al_2Si_6O_{18}$	$BeAl_2O_4$	$BeAl_6O_{10}$
Luminescence range/nm	650 – 1050	630 – 950	650 – 1050	620 – 1150
Wavelength of the luminescence maximum/nm	780	730	760	770, 900
Metastable-level lifetime τ/μs:				
$T = 77$ K	6.0	5.2	7.5	3.2
$T = 300$ K	4.5	1.0	5.0	1.7
Transition cross section $\sigma/10^{-19}$ cm^2	1.96	4.54	2.14	2.39
Wavelength at the maximum of the amplification band λ/nm	815	740	780	905
Width of amplification band $\Delta\nu$/cm^{-1}	3300	2500	3300	4600
Lasing range $\Delta\lambda$/nm	–	–	710 – 1070	–
Limiting radiation intensity I_m/T W cm^{-2}	150	47	130	210

beryllium aluminates doped with titanium ions were grown with significant growth defects, which precluded conducting experiments on the stimulated emission. Fig. 9 shows tunable outputs of $Ti^{3+}:Al_2O_3$ and $Ti^{3+}:BeAl_2O_4$ lasers obtained under similar conditions. In both cases, the same three-mirror V-shaped cavity was used with a Lyot filter as the tuning element. The active media were pumped by an argon laser (at 488 and 514.5 nm). One can see that the maximum of the amplification band of the $Ti:BeAl_2O_4$ crystal laser is shifted by 29 nm to the red as compared to that of the $Ti:Al_2O_3$ laser, as expected according to the single configurational coordinate model.

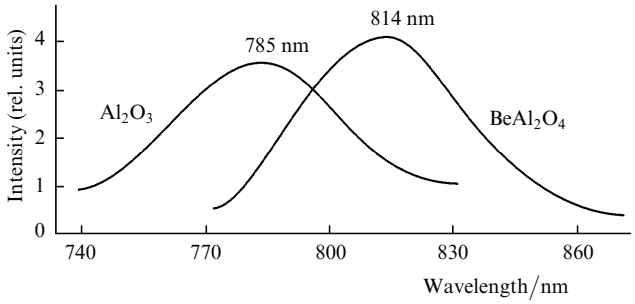

Figure 9. Emission spectra of cw $Ti^{3+}:Al_2O_3$ and $Ti^{3+}:BeAl_6O_{10}$ lasers.

Femtosecond pulses in the $Ti:BeAl_2O_4$ laser were generated in the traditional way using a Z-shaped cavity with a compensation for dispersion by two TF-8 glass prisms. A Kerr-lens mode-locking with a pulse duration of 75 fs was realised with a 15-mm long crystal pumped by an argon laser. When crystals of higher optical quality are employed, the amplification band of $Ti:BeAl_2O_4$ permits obtaining pulses shorter than 10 fs [25].

4. Conclusions

Therefore, the $Ti:BeAl_2O_4$ crystal is the second active medium in which stimulated emission of Ti^{3+} ions was obtained. The lasing was realised in the cw mode upon coherent pumping and a Kerr-lens mode-locking. As a laser medium, $Ti:BeAl_2O_4$ does not offer significant advantages over $Ti:Al_2O_3$, the lasing parameters of both active media being similar. The $Ti:BeAl_2O_4$ crystals may be used primarily in KML lasers, because the requirements imposed on the thermal physical characteristics in higher-power CPA laser systems are more stringent, and chrysoberyl ranks below sapphire in these parameters (see Table 1).

The $Ti:BeAl_6O_{10}$ crystal, which possesses an anomalously broad amplification band, is of great interest for the development of femtosecond laser systems. However, the use of this crystal is presently limited due to the drawbacks of the technology for growing crystals free from defects.

Among the laser media based on Cr^{3+}-doped beryllium-containing oxides, those that can be pumped by laser diodes emitting in the 650–670 nm region should be set aside. These are the $Cr:BeAl_2O_4$, $Cr:Be_3Al_2Si_6O_{18}$, and $Cr:BeAl_6O_{10}$ crystals, the $Cr:BeAl_6O_{10}$ crystal being the most convenient for diode pumping. A broad amplification band of this crystal of width 2600 cm^{-1} can provide, in the case of a Kerr-lens mode-locking, extremely short pulses of duration 4 fs.

In CPA laser systems, according to the experimental data obtained here, most attractive for use as active media are the $Cr:BeAl_2O_4$ and $Cr:BeAl_6O_{10}$ crystals. Both crystals exhibit excellent thermal physical properties and can be pumped by flashlamps or lasers. Estimates show that these crystals can be used for building high-power terawatt femtosecond laser systems.

Our investigations have demonstrated that beryllium aluminate crystals doped with titanium and chromium ions are promising media for the development of femtosecond KML and CPA laser systems. It is possible to design compact laser systems based on $Ti:BeAl_6O_{10}$, $Cr:BeAl_2O_4$, and $Cr:BeAl_6O_{10}$ crystals, which can produce femtosecond pulses and amplify them to terawatt intensities. Laser systems of this type open up broad possibilities for studies in the field of nonlinear optics of extremely short pulses and relativistic laser physics. They also can be used in chemistry, biology, medicine, and technology.

Acknowledgements. The authors thank S N Bagaev for his interest and support of this work, V V Petrov, V I Trunov, A V Kirpichnikov, A G Volkov, I I Zubrinov, and S V Bogdanov for their participation in the studies of physical, spectral, and lasing properties of the crystals, T A Matrosova and V I Alimpiev for their assistance in the crystal synthesis and growing, and A Ya Rodionov for providing beryl crystals grown by the gas-transport technique.

This work was partly supported by the Russian Foundation for Basic Research (Grant No. 01-02-16845), Siberian Division of the Russian Academy of Sciences (Project No. IG2000-8), and the 'Laser Physics' and 'Fundamental metrology' Programmes of the Russian Federation.

References

1. Sartania S, Sheng Z, Lenzner M, Tempea G, Spielmann Ch, Krausz F, Ferencz K *Opt. Lett.* **22** 1562 (1997)
2. Stickland D, Mourou G *Opt. Commun.* **56** 219 (1985)
3. Maine P, Stickland D, Bado P, Pessot M, Mourou G *IEEE J. Quantum Electron.* **24** 398 (1988)
4. Backus S, Durfee III Ch, Murnaine M, Kapteyn H C *Rev. Sci. Instrum.* **69** 1207 (1998)
5. Walker B C, Toth C, Fittinghoff D N, Guo T, Kim D, Rose-Petruck Ch, Squier J A, Yamakana K, Wilson K R, Barty C P J *Opt. Express* **5** 196 (1999)
6. Bonlia J D, Patterson E, Price D, White B, Springer P *Appl. Phys. B* **70** S155 (2000)
7. Moulton P F *Proc. IEEE* **80** 348 (1992); *J. Opt. Soc. Am. B: Opt. Phys.* **3** 125 (1986)
8. Hentshel M, Cheng Z, Krausz F, Spielmann Ch *Appl. Phys. B* **70** S161 (2000)
9. Bagnound V, Salin F *Appl. Phys. B* **70** S165 (2000)
10. Janusauskaus G, Oberle J, Rulliere C *Opt. Lett.* **23** 918 (1998)
11. Togashi T, Nabekawa Y, Sekikawa T, Nagasawa Y, Watanabe S *Appl. Phys. B* **60** 169 (1999)
12. Beaud P, Richardson M, Miesak E *IEEE J. Quantum Electron.* **31** 317 (1995)
13. Korf D, Weingarten K J, Zhang G, Moser M, Emanuel M, Beach R J, Skidmore J A, Keller U *Appl. Phys. B* **65** 235 (1997)
14. Honninger C, Paschotta R, Graf M, Morier-Genoud F, Zhang G, Moser M, Biswal S, Braun A, Mourou G A, Johannsen I, Giesen A, Seeber W, Keller U *Appl. Phys. B* **69** 3 (1999)
15. Spence D E, Kean P N, Sibbett W *Opt. Lett.* **16** 42 (1991)
16. Krausz F, Fermann M E, Brabec T, Curley P F, Hofer M, Ober M H, Spielmann Ch, Winter E, Schmidt A I *IEEE J. Quantum Electron.* **28** 2097 (1992)
17. Haus H A, Fujimoto J G, Ippen E P *IEEE J. Quantum Electron.* **28** 2086 (1992)

18. Kalashnikov I L, Krimer D O, Poloiko I G *Kvantovaya Elektron.* **30** 927 (2000) [*Quantum Electron*. **30** 927 (2000)]
19. Komarov A K, Komarov K P *Opt. Commun.* **183** 265 (2000)
20. Di Bartolo B *Optical Interactions in Solids* (New York\!:\! Wiley, 1968)
21. Petermann K *Opt. Quantum Electron.* **22** 199 (1990)
22. Mourou G *Appl. Phys. B* **65** 205 (1997)
23. *Fizika i spektroskopiya lazernykh kristallov* (Physics and Spectroscopy of Laser Crystals) A A Kaminskii (Ed.) (Moscow\!:\! Nauka, 1986)
24. Kenyon P, Andrews L, McCollum B, Lempicki A *IEEE J. Quantum Electron*. **18** 1189 (1982)
25. Pestryakov E V, Petrov V V, Kirpichnikov A V, Trunov V I, Komarov K P, Alimpiev A I *Laser Phys.* **8** 612 (1998)
26. Krupke W F, Shinn M D, Marion J E, Caird J A, Stokowski S E *J. Opt. Soc. Am. B: Opt. Phys.* **3** 102 (1986)
27. Walling J C, Peterson O G, Jenssen H P, Morris R C, O'Dell E W *IEEE J. Quantum Electron.* **16** 1302 (1980)
28. Peicong P, Xiaoshan M, Zhiwei H *Cryst. Res. Technol.* **27** 321 (1992)
29. Pestryakov E V, Petrov V V, Zubrinov I I, Semenov V I, Trunov V I, Kirpichnikov A V, Alimpiev A I *J. Appl. Phys.* **82** 3661 (1997)
30. Alimpiev A I, Gulev V S, Mokruchnikov P V *Cryst. Res. Technol.* **30** 295 (1995)
31. Bersuker I B *Effekt Yana–Tellera i Vibronnye Vzaimodeistviya v Sovremennoi Khimii* (Jahn–Teller Effect and Vibronic Interactions in Modern Chemistry) (Moscow: Nauka, 1987)
32. Lifshits M G, Mishkel' Ya I, Tarasov A A *Kvantovaya Elektron.* **18** 1319 (1991) [*Sov. J. Quantum Electron*. **21** 1204 (1991)]
33. Sennaroglu A *Opt. Commun.* **174** 215 (2000)
34. Chassagne B, Ivanov A, Rulliere C *Opt. Commun.* **141** 69 (1997)
35. Penzkofer A *Prog. Quantum Electron.* **12** 291 (1988)